J. ADV. SIMULAT. SCI. ENG.
Vol. 10, No. 1, 132-143.

Molecular Dynamics Simulation on Hydrogen Trapping on Tungsten Vacancy

Hiroaki Nakamura[1,2,*], Kazuki Takasan[2,†], Miyuki Yajima[1], Seiki Saito[1,3]

[1]National Institute for Fusion Science
[2]Nagoya University
[3]Yamagata University

[*]hnakamura@nifs.ac.jp, [†]present affiliation: Shiga University

Received: December 29, 2022; Accepted: April 17, 2023; Published: April 25, 2023

Abstract. The effect of hydrogen on the structural change of vacancies in tungsten is analyzed by molecular dynamics in order to clarify the interaction between vacancies and hydrogen in tungsten. Simulations are performed at different temperatures (573, 773, 1073 K) and with different numbers of hydrogen in the vacancies (0, 18, 36, 54). Evaluating (1) isopotential surface for the increase of total potential energy, (2) the root mean square deviation (RMSD) of tungsten atoms, (3) the root mean square fluctuation (RMSF) of tungsten atoms and (4) density distribution in radial direction, we found that the presence of a large number of hydrogen in a vacancy at each temperature caused changes in the structure. This fact partially supports the experimental fact that in the coalescence of two tungsten vacancies, the retention of hydrogen activates them.

Keywords: Molecular dynamics, tungsten, hydrogen, vacancy

1. Introduction

In magnetic confinement fusion, the plasma is confined in a "cage" made of magnetic field lines, and the high-temperature, high-density plasma floats in a vacuum vessel. The outermost magnetic-field surface where the magnetic field lines interweave without contacting the solid wall is called the separatrix. The plasma is divided into three layers: the core plasma inside the separatrix, the peripheral plasma near the separatrix, and the scrape-off layer (SOL) where the magnetic field lines intersect the solid wall. Plasma particles from the core to the SOL region are transported mainly along magnetic field lines and flow into the divertor plates. Since transport across the magnetic field lines is much smaller than transport along the field lines, the heat flow passes from the core plasma to near the separatrix and eventually flows into the divertor plates. Its heat flux density is estimated to reach 10 MW/m^2. Tungsten (W) with its high melting point and thermal conductivity is one of the most promising candidates for plasma facing materials including a divertor plate. In

addition, W has lower hydrogen isotope solubility than carbon materials and is less prone to wear and tear due to hydrogen isotopes. On the other hand, defects such as atomic vacancies and voids in metals are known to act as trapping sites for hydrogen isotopes, and it has been suggested that tritium (T) retention may be increased by neutron irradiation, which is a product of nuclear fusion.

Because hydrogen isotopes contain tritium, which is a radioactive material, this retention is limited in fusion reactor operation. Therefore, it is necessary to control this retention in the steady-state operation of fusion reactors. Elucidating the interaction between tungsten, vacancies, and hydrogen isotopes is one of the key issues, and various studies have been conducted through numerical calculations and experiments. For example, there are ion and neutron irradiation experiments as shown in Refs. [1–5].

Experiments [6–8] and simulations such as positron annihilation spectroscopy [9], the first-principles calculations [10], and density functional theory (DFT) calculations [11, 12] have been performed to clarify the interaction between vacancies in W and hydrogen isotopes.

However, the effect of different exposure temperatures of hydrogen isotopes on the interaction between vacancies and hydrogen isotopes has not been fully elucidated. Therefore, the purpose of this study is to clarify the interaction effects between vacancies and hydrogen isotopes at different hydrogen isotope exposure temperatures using the Molecular dynamics (MD) simulation. To achieve the objective of this study, we developed the W-Hydrogen (H) code developed by the authors [12, 13] and performed simulations of neutron-irradiated W with and without hydrogen isotopes.

Specifically, the phenomenon discussed in this paper is a report on the effect of hydrogen content on the coalescence phenomenon of two tungsten vacancies recently discovered by Yajima et al [8]. In their report, they found experimentally that a pair of hydrogen-containing vacancies combine more easily than a pair of non-hydrogen-containing vacancies. The explanation for this dependence is not yet known. Therefore, we set our final goal to elucidate the effect of hydrogen content on the coalescence of vacancies by MD simulations. However, since we do not yet have the know-how to deal with the coalescence of vacancies, in this paper we first consider a single vacancy and investigate how the shape of the vacancy changes with the hydrogen content in the vacancy from the atomic level using MD simulation.

2. Simulation Model and Algorithm

We use the molecular dynamics (MD) simulation to calculate tungsten and hydrogen trajectories, which are interacted with each other by Wang's Embedded Atom Method (EAM) potential [13]. This simulation method is based on our previous work [12].

The total MD simulation time is 51 ps with a time step $\Delta t = 0.02$ fs which is divided into two times t regions, before and after 1 ps (see Fig. 1).

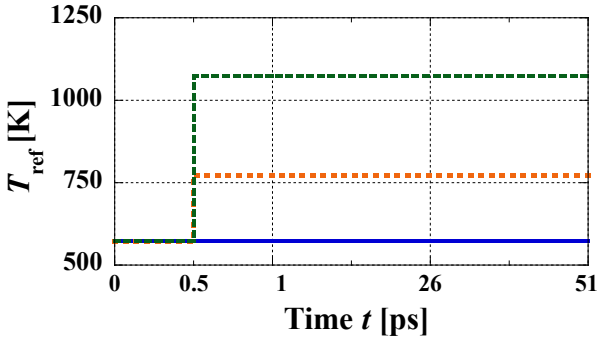

Figure 1: Time development of the reference temperature T_{ref}. As the initial configuration, the tungsten bcc crystal is arranged at $t = 0$. At $t = 0.5$ ps, a vacancy is created by removing 9 tungsten atoms from the bcc crystal. Then n hydrogen atoms are packed randomly into the vacancy at $t = 1$ ps. The total process of the MD simulation is divided into two processes, (i) the preparatory process $0 \leq t \leq 1$ ps, and (ii) the main process 1 ps $< t \leq 51$ ps. During the whole simulation, the time step $\Delta t = 0.02$ fs.

2.1. Preparatory process; $0 \leq t \leq 1$ ps

No vacancies are present in this process. Tungsten atoms are arranged in a perfect bcc crystal arrangement with a lattice constant a, where $a = 3.16$ Å. The volume of the crystal is $15a \times 15a \times 15a$, and the number of tungsten atoms is 6,750 atoms. The periodic boundary conditions are imposed in the x, y and z directions during the entire period of the MD simulation, 0 ps $\leq t \leq 51$ ps. From the initial tungsten structure arranged in this way, the tungsten crystal is heated under the NVT ensemble, *i.e.,* the canonical ensemble in order to create a stable state up to $t = 0.5$ ps. In this MD simulation, the temperature is controlled with the Langevin heat bath as the reference temperature 300 K.

Next, we create a vacancy by removing the nine tungsten atoms that are in the unit lattice corresponding to the center of the tungsten structure obtained at 0.5 ps, as shown in Fig. 2. The MD simulation is then resumed and calculated up to $t = 1$ ps under the NVT ensemble with the Langevin heat bath as the reference temperature T_{ref}, where we used $T_{\mathrm{ref}} = 573, 773$, or 1073 K, respectively.

2.2. Main process; 1 ps $< t \leq 51$ ps

As shown in Fig. 3, n hydrogen atoms are filled randomly into the vacancy, where we choose $n = 0$, 18, 36 and 54. To make MD calculations more realistic, the region where tungsten atoms are present is divided into a brown mesh region (NVT region) and a green dotted region (NVE region) in Fig. 2 (b). This region dividing method is the same technique used in our previous work [12]. In the NVT region, the temperature is controlled with the Langevin heat bath as the reference temperature T_{ref} as same as in the preparatory process of §2.1. In the NVE regime, on the other hand, the equations of motion for all atoms are solved numerically under the NVE ensemble *i.e.,* the microcanonical ensemble in which

the total energy is conserved without applying a heat bath. The size of the NVE region is $5a \times 5a \times 5a$. The vacancy with n hydrogen atoms is located in the center of the NVE region as it had been while 0.5 ps $\leq t \leq$ 1 ps.

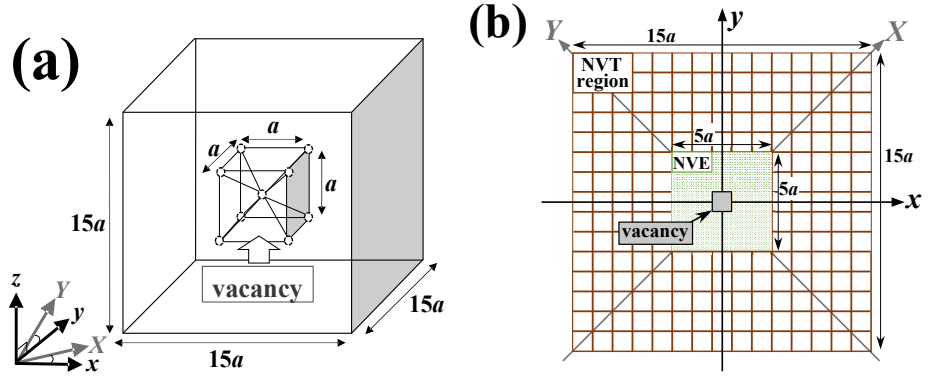

Figure 2: The simulation model in the main process 1 ps $< t \leq$ 51 ps. (a) A tungsten bcc crystal with the size $15a \times 15a \times 15a$ is set as the simulation model, where the lattice constant a = 3.16 Å. A vacancy with the size $a \times a \times a$ is prepared by removing 9 tungsten atoms located in the center of the crystal. Into the vacancy, n hydrogen atoms are packed, where we consider the cases of $n = 0, 18, 36, 54$. A cross-sectional view in the $xy-$plane is shown in (b), where the vacancy is shown as a gray-filled square. The region where tungsten atoms are present is divided into a brown mesh region (NVT region) and a green dotted region (NVE region). In the MD simulations, the temperature of the NVT region is controlled with the Langevin heat bath as the reference temperature T_{ref}, where we used $T_{\mathrm{ref}} = 573, 773, 1073$ K. The size of the NVE region is $5a \times 5a \times 5a$. The periodic boundary conditions are applied to this simulation box in the x, y and z directions. The new coordinate system which is the xyz coordinate system rotated $+\pi/4$ around the z axis is defined as the XYZ coordinate system, where the Z axis is the same as the z axis.

3. Simulation Results and Discussions

As mentioned at the end of §1., the purpose of this paper is to clarify Yajima's experimental result that, in the coalescence of two tungsten vacancies, the reaction is more active when the vacancies contain hydrogen. Since our current simulations cannot handle the coalescence of two vacancies, the simulations in this paper are intended to provide a clue to the cause of Yajima's experiment by investigating the dependence of the change in the shape of one vacancy on the amount of hydrogen contained in the vacancy.

We performed a total of 12 MD simulations in the main process as a result of changing the reference temperature and the number of hydrogen atoms, *i.e.,* T_{ref} = 573, 773, 1073 K, and n = 0, 18, 36, 54.

To investigate how the size of the vacancy changes with the number of hydrogen contents n in the vacancy, we extract the four physical quantities, (1) the isopotential surface for the increase of total potential energy, (2) the root mean square deviation (RMSD) of W atoms,

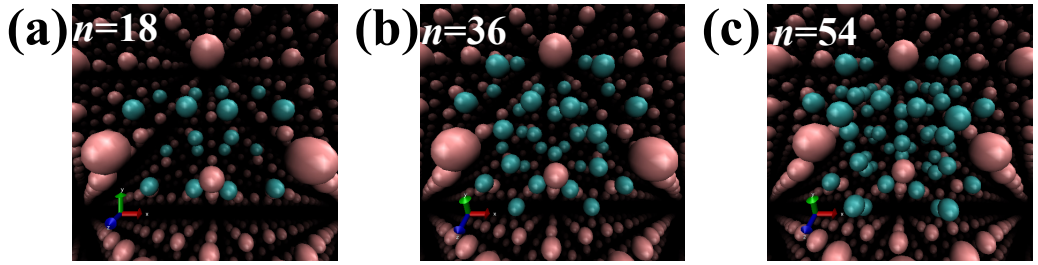

Figure 3: At $t = 1$ ps, n hydrogen atoms are packed into the vacancy; (a) $n = 18$, (b) $n = 36$ and (c) $n = 54$. The blue and peach balls represent hydrogen and tungsten atoms, respectively.

(3) the root mean square fluctuation (RMSF) of W atoms and (4) density distribution in the radial direction.

In each of the following subsections, we will define each physical quantity and explain the significance of obtaining it. Furthermore, by actually evaluating these physical quantities, we will report how the shape of a single vacancy changes with the amount n of hydrogen contained in it, which is the purpose of this paper.

3.1. Isopotential surface for the increase of total potential energy

We can determine the stability of the vacancy for a given number n of contained hydrogen atoms by examining the n-dependence of the Helmholtz free energy. However, since it is difficult to accurately determine the Helmholtz free energy here, we will substitute an evaluation of the potential energy. We comment on the fact that we use the potential energy instead of the free energy. At zero temperature the two coincide, but at finite temperature, there is a difference. In other words, we need to consider entropy at finite temperatures. However, the temperature T_{ref} we are dealing with here is between 573K and 1073K, which is below the melting point of tungsten (3695K), so we can assume that tungsten is retained in the solid state. Therefore, we expected to capture the characteristics of the vacancy shape and the atomic distribution by evaluating the potential energy at each position.

Moreover, in order to evaluate the stability of the shape of the vacancy, we focus on the ease of movement of tungsten atoms adjacent to the vacancy. In other words, we consider that by examining the distribution of the potential increment within the vacancy, we can indirectly evaluate the force applied to the tungsten around the vacancy.

In addition, as a direct evaluation of the fluctuations of tungsten atoms, we evaluate the root mean square deviation (RMSD) and the root mean square fluctuation (RMSF) in §3.2. and §3.3., respectively.

The distribution of the increase in the total potential energy for the addition of one more hydrogen atom named “probe hydrogen” to a tungsten vacancy filled with n hydrogen atoms, depending on the position of the probe hydrogen $\boldsymbol{r}_{\mathrm{prob}}$, is depicted in Fig. 4. Here is an explanation for the probe hydrogen: the MD simulation is calculated under N particles. The probe hydrogen is added at the position $\boldsymbol{r}_{\mathrm{prob}}$, and the potential energy among (N +

1) particles is calculated. However, the time evolution of these $(N + 1)$ particles is not calculated. The potential energy increase $\Delta U(\boldsymbol{r}_{\mathrm{prob}})$ at each position $\boldsymbol{r}_{\mathrm{prob}}$ is ~~determined~~ defined as follows.

$$\Delta U(\boldsymbol{r}_{\mathrm{prob}};\, \{\bar{\boldsymbol{r}}\}) := U_{N+1}(\{\bar{\boldsymbol{r}}\}) - U_N(\{\bar{\boldsymbol{r}}\}), \tag{1}$$

where N is the total number of atoms in the tungsten material with a vacancy containing n hydrogen atoms before adding the probe hydrogen, and $\{\boldsymbol{r}\}$ denotes the set of the position of all atoms in the tungsten material excluding the probe hydrogen. Here, " $\bar{}$ " means the time average while 50 ps $< t \leq$ 51 ps. The total potential energy of the N atoms is defined by U_N. Therefore, $U_N(\{\bar{\boldsymbol{r}}\})$ is the total potential energy before adding the probe hydrogen; $U_{N+1}(\{\bar{\boldsymbol{r}}\})$ is the total potential energy after adding the probe hydrogen.

In our analysis (1), we are calculating the potential energy when the particles are placed in time-averaged positions $\{\bar{\boldsymbol{r}}\}$, rather than the time-averaged value of $\overline{U_N}$ itself. The reasons for this are as follows: (i) The shape of the vacancy can be easily determined by using the time-averaged position of each particle $\{\bar{\boldsymbol{r}}\}$. (ii) The potential energies $U_N(\{\bar{\boldsymbol{r}}\})$ and $U_{N+1}(\boldsymbol{r}_{\mathrm{prob}};\, \{\bar{\boldsymbol{r}}\})$ can then be easily calculated.

On the other hand, if the time average of the potential $\overline{U_N}$ is used, it is difficult to identify the shape of the vacancy because each atom moves. Furthermore, if one additional probe hydrogen is added, the time evolution must be further calculated, complicating the analysis. For these reasons, we chose to calculate the spatial distribution of the potential energy increments using average coordinates, *i.e.*, $U_N(\{\bar{\boldsymbol{r}}\})$.

By using this distribution map, *i.e.,* the isopotential surface Fig.4, the location of the ease of hydrogen packing can be identified. For $n = 0$ and 18, the negative ΔU region (blue region) exists in the vacancy as shown in Fig.4 (a) and (b). It means that hydrogen atoms can be stably added to this blue region. However, for $n = 36$ and 54, the blue region disappears even in the vacancy. Especially, ΔU becomes a large value in about half of the vacancy for $n = 54$, which means that forcing hydrogen to fill the vacancy increases the likelihood of recoil of nearby tungsten atoms, especially for $n = 54$.

3.2. Root mean square deviation (RMSD) of tungsten atoms

Next, the root mean square deviation (RMSD) is used to calculate the time evolution of the migration of tungsten atoms from the structure at a given time. The RMSD is defined as follows:

$$RMSD(t) := \sqrt{\frac{1}{N_{\mathrm{W}}} \sum_{i=1}^{N_{\mathrm{W}}} |\boldsymbol{r}_i(t) - \boldsymbol{r}_i(t_0)|^2}, \tag{2}$$

where $t_0 = 1$ ps and $\boldsymbol{r}_i$ is the position of the tungsten atom i, for $1 \leq i \leq N_w$ at time t. Here N_{W} is the number of the tungsten atoms. We plot the time dependence of RMSD for all n at T_{ref} in Fig.5. Moreover, the time averages of $RMSD$ during the period of 20 ps $\leq t \leq$ 51 ps are shown in Fig. 6. Focusing on the difference by the T_{ref}, it is found that the larger the value of T, the larger the time average of $RMSD$. In terms of differences by n, there are little differences between $n = 0$, 18, and 36 for any T. On the other hand, for $n = 54$, there was an increase in $RMSD$, unlike for the other n. At $T = 573$ K and 773 K, the $RMSD$ increased by about 0.02 Å compared to $n = 0$, 18, and 36. At $T = 1073$ K, it was about 0.01 Å higher

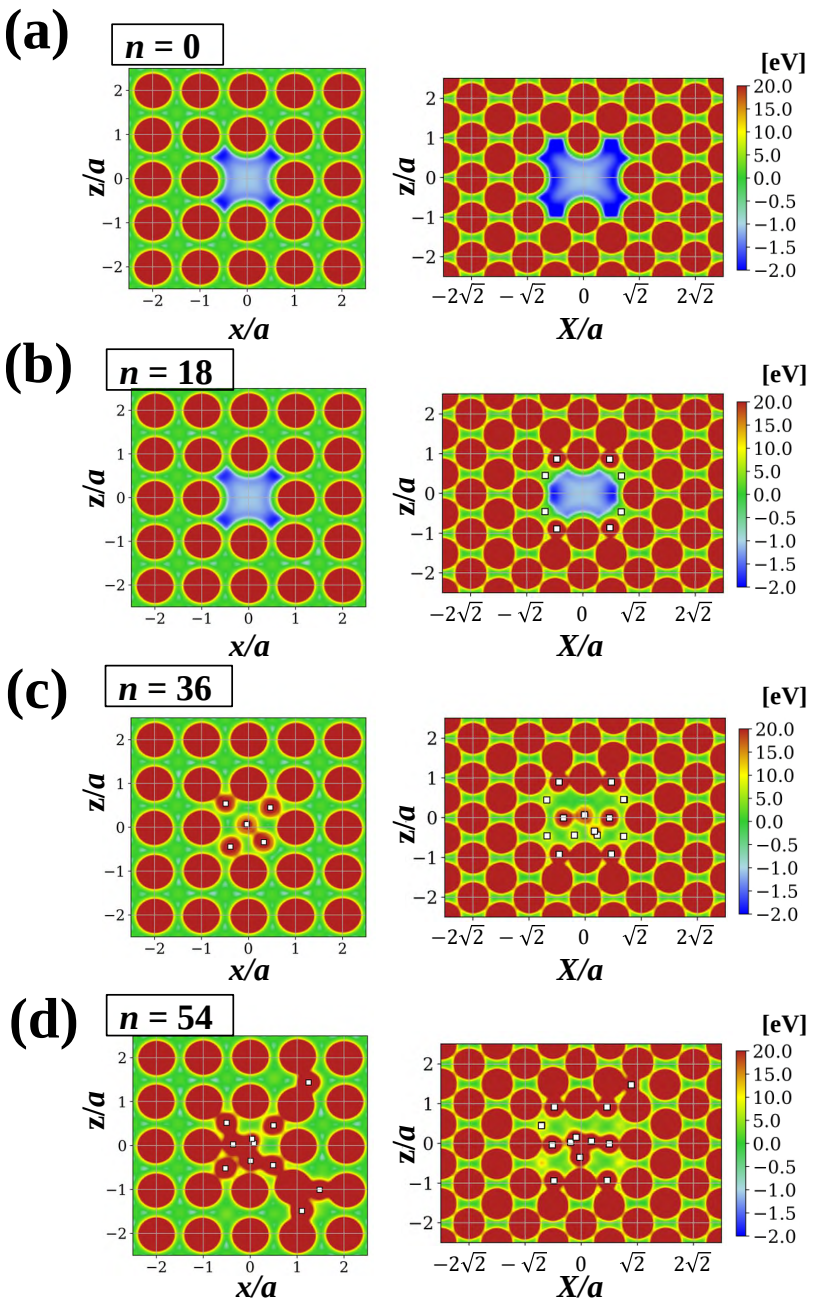

Figure 4: The isopotential surface of $\Delta U(\boldsymbol{r}_{\mathrm{prob}}; \{\bar{\boldsymbol{r}}\})$, where $\boldsymbol{r}_{\mathrm{prob}}$ are in the $y = 0$ cross section (the xz plane) or in the $Y = 0$ cross section (the Xz plane), is drawn on the right figures or the left figures, respectively. The number of hydrogens in the vacancy $n = 0$ (a), 18 (b), 36 (c), and 54 (d) and the reference temperature $T_{\mathrm{ref}} = 573$ K. The scale of all coordinates is normalized by the lattice constant a, which is 3.16 Å.

than at $n = 0$, 18, and 36. From these results, it is found that, when packing hydrogen into the vacancy, the n dependence was previously unfamiliar, but as n increases to about 54, the RMSD becomes larger. This means that by packing a lot of hydrogen into the vacancy, the surrounding tungsten is under force and moving.

3.3. Root mean square fluctuation (RMSF) of tungsten atoms

Third, the root mean square fluctuation (RMSF) of the tungsten atom is calculated to evaluate the fluctuation of the tungsten atom. By examining this physical quantity, we can evaluate whether the shape of the vacancy is susceptible to change. The RMSF is defined by

$$\mathrm{RMSF} := \sqrt{\frac{1}{N_\mathrm{W}} \sum_{i=1}^{N_\mathrm{W}} \overline{\left| \boldsymbol{r}_i(t) - \overline{\boldsymbol{r}_i(t)} \right|^2}}, \tag{3}$$

"$\overline{\ }$" means the time average while 50 ps $< t \leq$ 51 ps as same as in §3.1. We plot the RMSF for n and T_ref in Fig.7. From this figure, it is found that, in terms of differences by n, there are little differences between $n = 0$, 18, and 36 for any T and that, there was an increase in $RMSF$ for $n = 54$, unlike for the other n. This n-dependence of RMSF is similar to the time average of RMSD in Fig.6. This indicates that, as in the previous analysis, the tungsten atoms are shaken by the large amount of hydrogen packed in the vacancies. Conversely, the shape of the vacancies is easily changed.

3.4. Density distribution in radial direction

Finally, we will examine how hydrogen filling the vacancies the crystallinity of tungsten is disrupted by the filling of vacancies with hydrogen. To evaluate the disorder of the tungsten crystal structure, the density distribution ρ of tungsten atoms in the radial direction from the origin is calculated using the following definition.

$$\rho(r) := \frac{\overline{n_\mathrm{W}}(r)}{\Delta V(r)}, \tag{4}$$

where $\overline{n_\mathrm{W}(r)}$ is the time-averaged number of tungsten atoms within a radius $r + \Delta r$ from the origin during 50 ps $< t \leq$ 51 ps as same as in §3.1. and $\Delta r = 0.1$Å. Moreover, the incremental volume of sphere ΔV in the denominator of Eq.4 is defined as

$$\Delta V(r) := \frac{4}{3}\pi(r + \Delta r)^3 - \frac{4}{3}\pi r^3. \tag{5}$$

For each n and T_ref, $\rho(r)$ is plotted in Fig.8. From this figure, we can find peak shapes that reflect the crystal structure of tungsten. It can be seen that the overall peak height decreases as the temperature increases. Next, focusing on the first peak around $r \sim a = 3.14$ Å at each temperature, it is also found that as n increases, the peak height decreases and the width of the peak widens slightly. These results suggest that the crystal structure tends to be disrupted as the temperature increases and n increases. In other words, the shape of the vacancy formed by tungsten is disrupted with higher temperature or larger n.

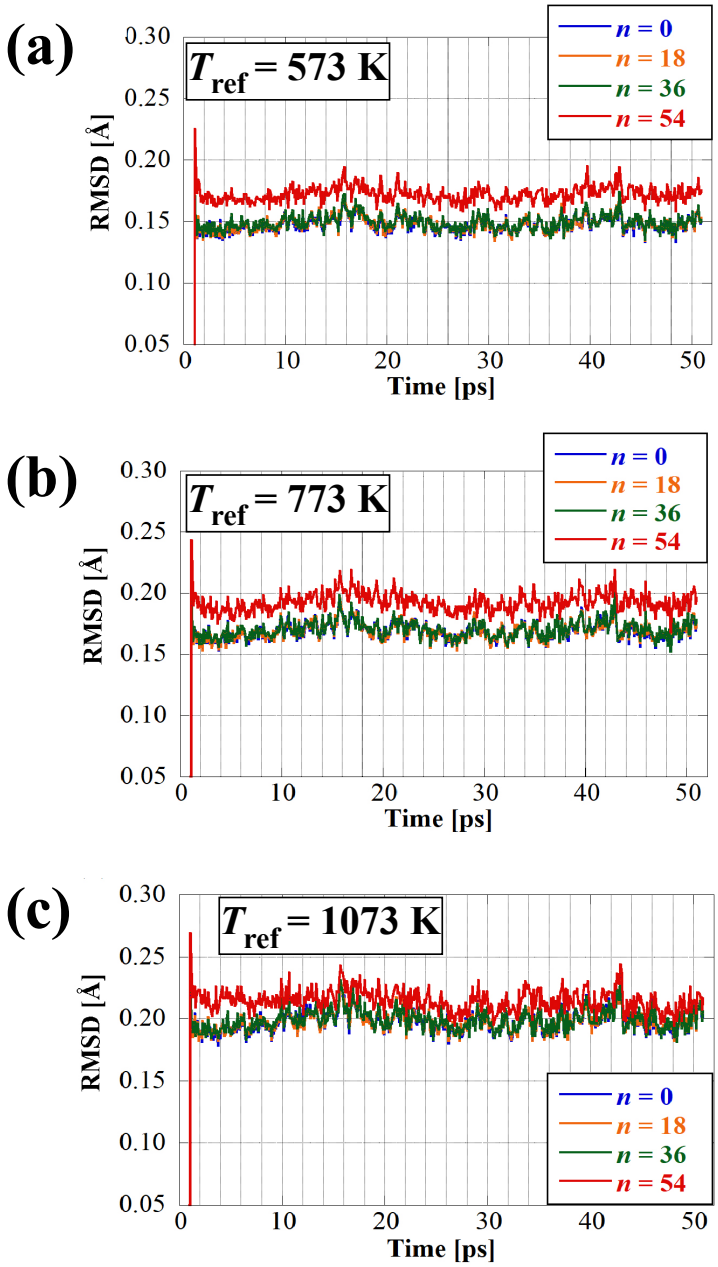

Figure 5: Time evolution of the root mean square deviation (RMSD) for tungsten atoms for $n = 0, 18, 36$ and 54 at the reference temperature $T_{\mathrm{ref}} = 573$ K (a), 773 K (b) or 1073 K (c), respectively. The parameter n means the number of hydrogen atoms in a vacancy.

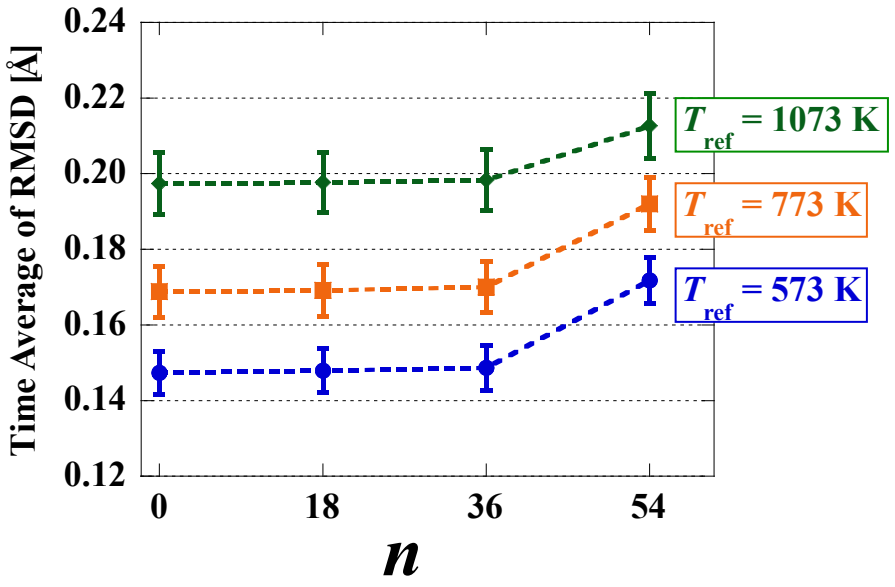

Figure 6: Time averages of the root mean square deviation (RMSD) for tungsten atoms for $n = 0, 18, 36$ and 54 at the reference temperatures $T_{\mathrm{ref}} = 573$ K (blue), 773 K (orange) and 1073 K (green). The error bars represent the standard deviation. The parameter n means the number of hydrogen atoms in a vacancy.

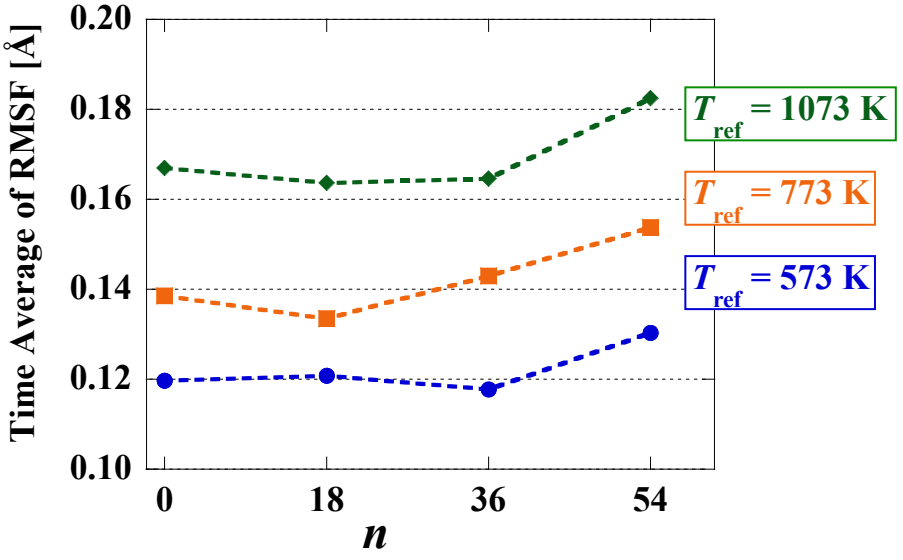

Figure 7: The root mean square fluctuation (RMSF) of tungsten atoms within 10 Å of the center of the vacancy at $t = 50$ ps is selected for each (n, T_{ref}), where $n = 0$, 18, 36, 54 and $T_{\mathrm{ref}} = 573$ K (blue), 773 K (orange) and 1073 K (green). At all T_{ref}, the RMSF for $n = 54$ is significantly greater than those for the other n.

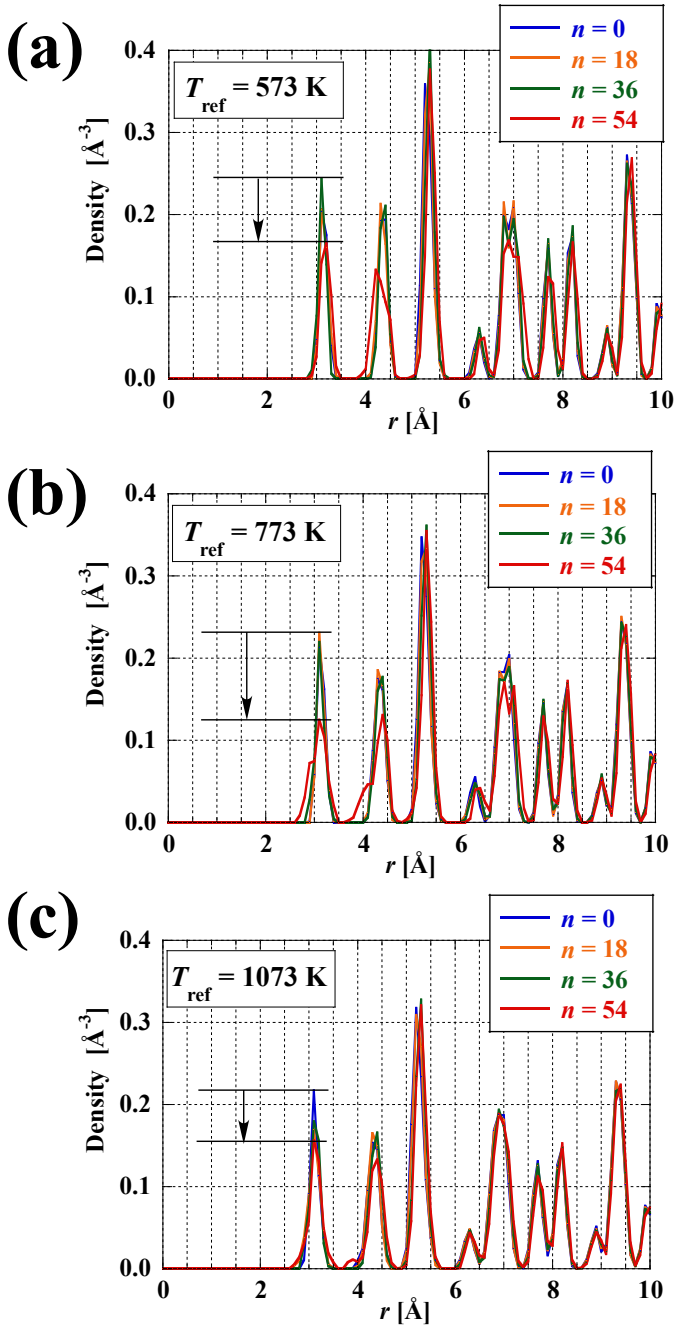

Figure 8: Density distribution of tungsten atoms in the radial direction in the cases of n = 0, 18, 36 and 54 at the reference temperatures T_{ref} = 573 K (a), 773 K (b) and 1073 K (c), respectively. As n becomes larger, the value of the first peak becomes smaller at all T_{ref}.

4. Conclusion

The effect of hydrogen on the structural change of vacancy in tungsten was analyzed by molecular dynamics in order to clarify the interaction between vacancy and hydrogen in tungsten. The results show that in the temperature range of 500 K to 1000 K, hydrogen filling of a tungsten vacancy, regardless of temperature, tends to change the shape of the vacancy. This fact partially supports Yajima's experimental fact that in the coalescence of two tungsten vacancies, the retention of hydrogen activates them.

Acknowledgments

The research was supported by JSPS KAKENHI Grant Numbers Nos. JP19K14692, JP19K03800, JP21K19845, JP22K03572, and JP23K03362 from the Japan Society for the Promotion of Science, and by the NIFS Collaborative Research Programs NIFS21KEMF182, NIFS22KIIP003 and NIFS22KISS021.

References

[1] B. Tyburska et al., J. Nucl. Mater., **395**, 150 (1992).

[2] J. Roth and K. Schmid, Phys. Scripta **T145**, 014031(2011).

[3] V. Kh. Alimov et al., J. Nucl. Mater., **441**, 280(2013).

[4] Y. Hatano et al., Mater. Trans., **54**, 437 (2013).

[5] Y. Oya et al., J. Nucl. Mater., **461**, 336 (2015).

[6] M. Yajima et al., Fusion Eng. Des., **21**, 100699(2019).

[7] V. Kh. Alimov et al., Nucl. Fusion, **60**, 096025(2020).

[8] M. Yajima et al., Phys. Scr., **96**, 4042 (2021).

[9] K. Ohsawa et al., J. Nucl. Mater., **527**, 151825(2019).

[10] D. Kato et al., Nucl. Fusion, **55**, 083019(2015).

[11] A. Takayama et al., J. Nucl. Mater., **463**, 355 (2015).

[12] S. Saito et al., J. Appl. Phys., **60**, SAAB08(2021).

[13] L.-F. Wang et al., Condens. Matter, **29**, 435401(2017).